

# The activity phase of postsynaptic neurons in a simplified rhythmic network

A. Bose<sup>(1)</sup>, Y. Manor<sup>(2)</sup>, and F. Nadim<sup>(1,3)</sup>

<sup>(1)</sup> Department of Mathematical Sciences and  
Center for Applied Mathematics and Statistics  
New Jersey Institute of Technology, Newark, NJ 07102

<sup>(2)</sup> Life Sciences Department  
Ben-Gurion University of Negov and  
Zlotowski Center for Neuroscience  
Beer-Sheva, Israel 84105

<sup>(3)</sup> Department of Biological Sciences  
Rutgers University, Newark 07102

CAMS Report 0304-26, Spring 2004

**Center for Applied Mathematics and Statistics**

**NJIT**

# The activity phase of postsynaptic neurons in a simplified rhythmic network

**Amitabha Bose**

Department of Mathematical Sciences, New Jersey Institute of Technology, Newark, NJ 07102  
Email: bose@njit.edu

**Yair Manor**

Life Sciences Department, Ben-Gurion University of the Negev and Zlotowski Center for  
Neuroscience, Beer-Sheva, Israel 84105  
Email: yairman@bgumail.bgu.ac.il

**Farzan Nadim**

Department of Mathematical Sciences, New Jersey Institute of Technology, Newark, NJ 07102 and  
Department of Biological Sciences, Rutgers University, Newark, NJ 07102  
Email: farzan@njit.edu

## Abstract

Many inhibitory rhythmic networks produce activity in a range of frequencies. The relative phase of activity between neurons in these networks is often a determinant of the network output. This relative phase is determined by the interaction between synaptic inputs to the neurons and their intrinsic properties. We show, in a simplified network consisting of an oscillator inhibiting a follower neuron, how the interaction between synaptic depression and a transient potassium current in the follower neuron determines the activity phase of this neuron. We derive a mathematical expression to determine at what phase of the oscillation the follower neuron becomes active. This expression can be used to understand which parameters determine the phase of activity of the follower as the frequency of the oscillator is changed. We show that in the presence of synaptic depression, there can be three distinct frequency intervals, in which the phase of the follower neuron is determined by different sets of parameters. Alternatively, when the synapse is not depressing, only one set of parameters determines the phase of activity at all frequencies.

# 1 Introduction

Many behaviors result from rhythmic activity of neuronal networks in which different groups of neurons are active at different times during the rhythm cycle. In most cases, such rhythms operate in a wide range of frequencies (Marder and Calabrese, 1996). In order for the network to produce a meaningful output, there needs to be a coordination between the activity patterns of these groups. For example, irrespective of frequency, different neurons may fire with a fixed latency, or a fixed phase, with respect to each other (Ahissar et al., 2000; Bartos et al., 1999). In other cases, the timing of activity may be a combination of these two relationships (Hooper, 1997a,b; Pearson and Iles, 1970).

Typically one might expect a fixed latency between the firing of the pre- and the postsynaptic neuron, independent of the activation frequency of the synapse (DiCaprio et al., 1997). It is less clear how two neurons could have a prescribed phase difference, independent of frequency, because the mechanism responsible for this temporal relationship would need continuous access to the rhythm frequency. Such a mechanism, if it exists, could be either externally imposed on, or emerge as a built-in property of the network. A recent computational study proposed that the dynamics of a synapse could be used to automatically set the phase between two neurons (Manor et al., 2003). This study demonstrated that a depressing inhibitory synapse between an oscillator and a follower neuron could produce a fixed phase difference between the two neurons across a relatively wide range of frequencies. The mechanism proposed by Manor et al. (2003) depended only upon the dynamics of the synapse and did not take account of other built-in elements such as intrinsic properties of the follower neuron. However, as demonstrated in previous studies, intrinsic currents may also be involved in delaying or advancing the onset of activity in follower neurons (Harris-Warrick et al., 1995).

In this work we study how synaptic and intrinsic dynamics interact to determine phase in a simple oscillator-follower network. In particular, we investigate the interplay between a depressing inhibitory synapse and a transient potassium ( $A$ ) current in the follower neuron. We choose to focus on the  $A$  current because it has been shown to play a significant role in timing the activity of neurons on rebound from synaptic inhibition (Harris-Warrick et al., 1995; Hess and Manira, 2001; Hsiao and Chandler, 1995). The  $A$  current is only one of several intrinsic currents that may contribute to the activity phase of the follower neuron. The analysis and insights of this work can be applied to understand the contribution of other types of currents, such as the hyperpolarization-activated inward current or a low-threshold calcium current.

The model we study consists of a simplified network in which the presynaptic neuron is simply a square-wave oscillator and the follower is a generic two-variable excitable neuron, modified by adding an  $A$  current. The small number of variables in this model enables us to use phase-plane analysis to derive a mathematical expression for the phase difference between the oscillator and the follower neuron. The mathematical techniques provide a novel way to incorporate the effects of the  $A$  current in a phase plane model. Moreover, this analytical approach allows us to pinpoint the parameters that most significantly affect phase in different frequency domains.

We find that, with a non-depressing synapse, there is a fixed latency between the activity of the oscillator and the follower neuron, independent of frequency. In contrast, with the appropriate choice of parameters, a depressing synapse acts synergistically with the A current to control phase. In particular, we find that there can be three separate frequency intervals in which the phase of the follower neuron is determined by different and independent parameters. Thus, intrinsic properties in conjunction with synaptic dynamics can considerably extend the frequency range for which phase may be controlled.

## 2 Model and Equations

### 2.1 The oscillator neuron $O$

In this study we focus only on the effect of an oscillator neuron  $O$  inhibiting a follower neuron  $F$ . For simplicity, the activity of  $O$  is described by a periodic square wave pulse with voltage  $v_O$ . We denote the length of the active state of  $O$  ( $v_O > v_{thresh}$ ) by  $T_{act}$ , and the length of the inactive state ( $v_O < v_{thresh}$ ) by  $T_{inact}$ , where  $v_{thresh}$  denotes the threshold for synaptic transmission. The period of  $O$  is given by  $P = T_{act} + T_{inact}$ .

### 2.2 Intrinsic dynamics of the follower neuron $F$

The top trace of Fig. 1 shows a typical intracellular voltage trace of a follower PY neuron recorded from the crab pyloric nervous system entrained to follow a periodic stimulus (Nadim, unpublished data). The trace can be divided into three parts: spikes riding on top of a burst envelope, a low-voltage hyperpolarized state and an intermediate-voltage state leading up to the spiking activity. The periodic activity of the PY neuron *in vivo* results from synaptic inhibition that it receives from the pacemaker neurons of the pyloric network. In the trace shown in Fig. 1, this neuron is synaptically isolated and the input from the pacemaker neurons is replaced by a periodically injected negative current pulse. This PY neuron is a biological representative of the follower neuron  $F$  in this study. Our results focus on the (bursting) activity of the follower neuron while ignoring the exact timing of the individual spikes. As such, we shall approximate the activity of a bursting neuron with a voltage trace that smooths over the spikes (middle trace of Fig. 1). We shall keep track of two important time intervals related to the activity of  $F$ . The first is  $t_f$ ; it is the time that the follower neuron  $F$  stays in the low-voltage silent state. The second is  $t_a$ ; it is the time that the follower neuron  $F$  stays in the intermediate-voltage state. The main goal of this work is to derive analytical expressions for  $t_f$ ,  $t_a$  and phase ( $\phi = [t_f + t_a]/P$ ) as a function of the period  $P$  of the oscillator  $O$ .

The activity of the follower neuron  $F$  is governed by biophysical current balance equations. We begin with a simple 2-dimensional excitable neuronal model (such as a Morris-Lecar or Fitzhugh-Nagumo type neuron) that does not yet incorporate the A current. The activity of such a neuron

can be geometrically represented in a 2-dimensional phase plane with equations that produce a cubic shaped voltage nullcline (Rinzel and Ermentrout, 1997). We will not be concerned with the exact form of these equations, only with their qualitative dynamics. Thus, we present them in general form:

$$\begin{aligned}\epsilon v' &= f(v, w) \\ w' &= [w_\infty(v) - w]/\tau_w(v),\end{aligned}\tag{1}$$

where  $v$  represents the voltage of  $F$ ,  $w$  is the recovery variable and the derivative is with respect to time  $t$ . The  $v$ -nullcline  $\mathcal{C}_o = \{(v, w) : f(v, w) = 0\}$  is a cubic shaped curve, while the  $w$ -nullcline  $\mathcal{S}_o = \{(v, w) : w_\infty - w = 0\}$  is a sigmoidal shaped curve (Fig. 2A). The function  $f(v, w)$  is positive (negative) below (above)  $\mathcal{C}_o$ . We shall assume that  $\mathcal{C}_o$  and  $\mathcal{S}_o$  intersect at only one point  $(\hat{v}, \hat{w})$  where  $\hat{w} = w_\infty(\hat{v})$  along the right branch of  $\mathcal{C}_o$ , ensuring that the isolated  $F$  neuron has a stable, high voltage steady state. We denote the local minimum of  $\mathcal{C}_o$  by  $(v_{lk}, w_{lk})$ .

When  $\epsilon$  is small enough, equation (1) involves two distinct time scales (i.e., the system is singularly perturbed). These time scales control the trajectory of  $F$  in different regions of the phase space. The  $F$  trajectory can be divided into regions with slow movements at low- or high-voltage states and fast transitions between these states (Fig. 2). We will employ geometric singular perturbation theory to track the trajectory of  $F$  in the  $v - w$  phase plane (Mishchenko and Rozov, 1980). This involves deriving reduced (lower dimensional) sets of equations which govern the evolution of  $F$  along different parts of its trajectory. By setting  $\epsilon = 0$  in equation (1), we obtain the slow equations

$$\begin{aligned}0 &= f(v, w) \\ w' &= [w_\infty(v) - w]/\tau_w(v).\end{aligned}\tag{2}$$

The first equation forces  $F$  to lie on the  $\mathcal{C}_o$  nullcline. The second equation governs the evolution of  $w$  (and in turn  $v$ ) along  $\mathcal{C}_o$ . In particular, when  $F$  lies on the left branch of  $\mathcal{C}_o$ , then  $w' < 0$  and on the right branch  $w' > 0$ . By rescaling time  $t = \epsilon\xi$  and then setting  $\epsilon = 0$ , we obtain the fast equations (derivative below is with respect to  $\xi$ ).

$$\begin{aligned}\dot{v} &= f(v, w) \\ \dot{w} &= 0\end{aligned}\tag{3}$$

These equations govern fast transitions (or jumps) between the left and right branches of  $\mathcal{C}_o$ . A fast transition is a heteroclinic solution (connecting two critical points) of equation (3). For example, it may connect  $(v_{lk}, w_{lk})$  on the left branch of  $\mathcal{C}_o$  to a point  $(v_r, w_{lk})$  on the right branch of  $\mathcal{C}_o$ . The jumps between the silent and active states of  $F$  occur instantaneously with respect to the slow time  $t$  (Fig. 2). Fig. 2B shows the voltage trace of  $F$  corresponding to the trajectory shown in Fig. 2A. A neuron will said to be active if  $v > v_\theta$  (the trajectory of  $F$  lies on the right branch of  $\mathcal{C}_o$ ) and silent if  $v < v_\theta$  (the trajectory of  $F$  lies on the left branch of  $\mathcal{C}_o$ ), where  $v_\theta$  satisfies  $v_{lk} < v_\theta < \hat{v}$ .

For simplicity of the analysis, we assume that  $w_\infty$  is 0 for  $v$  values on the left branch of  $\mathcal{C}_o$ . We will also assume that the time constant  $\tau_w(v)$  of the recovery variable  $w$  assumes, respectively, the values  $\tau_L$  and  $\tau_R$  on the left and right branches of  $\mathcal{C}_o$ . These values determine the rate of evolution of  $F$  in its silent and active states (Fig. 2).

### 2.3 The $A$ current

The  $A$  current is modeled by  $I_A = \bar{g}_a a_m a_h [v - E_K]$ , where  $a_m$  and  $a_h$  respectively govern the activation and inactivation kinetics. The parameters  $\bar{g}_a$  and  $E_K$  are the maximal conductance and reversal potential of the  $A$  current. The inactivation variable  $a_h$  obeys the first order kinetic equation

$$a'_h = [h_\infty(v) - a_h]/\tau_h(v), \quad (4)$$

where  $h_\infty(v) = 1/[1 + \exp((v - v_m)/k_h)]$ . The parameter  $v_m$  should satisfy  $v_{lk} < v_m \leq v_\theta$  so that the  $A$  current recovers from inactivation on the left branch of the  $v$ -nullcline and starts to inactivate as soon as the  $F$  trajectory leaves the left branch. For simplicity of calculations we make a few assumptions. First, we assume that  $k_h \rightarrow 0$ , which will make the curve  $h_\infty$  a step function equal to 1 for  $v$  below  $v_m$  and 0 otherwise. Second, we also assume instantaneous all-or-none activation kinetics  $a_m = a_m(v) = H(v - v_\theta)$  where  $H$  is the Heaviside function.  $I_A$  recovers from inactivation when the  $F$  trajectory is on the left branch of the  $v$ -nullcline and inactivates otherwise. We will also assume that  $\tau_h(v)$  is equal to  $\tau_{lo}$  on the left branch of  $\mathcal{C}_o$ ,  $\tau_{hi}$  on the right branch of  $\mathcal{C}_o$  and  $\tau_{med}$  in a neighborhood of  $v = v_\theta$ . We assume that  $\tau_{hi}$  is sufficiently small so that  $a_h$  quickly decays toward 0 when  $v$  is large. With this assumption, there is no residual  $A$  current affecting the behavior of  $F$  when  $O$  becomes active again, making the calculations somewhat simpler.

The equations that govern the activity of  $F$  can now be written as

$$\begin{aligned} \epsilon v' &= f(v, w) - \bar{g}_a a_m a_h [v - E_K] \\ w' &= [w_\infty(v) - w]/\tau_w(v) \\ a'_h &= [h_\infty(v) - a_h]/\tau_h(v). \\ a_m &= H(v - v_\theta) \end{aligned} \quad (5)$$

We now define reduced equations which govern the evolution of  $F$  in different parts of its trajectory. When  $F$  is in the silent state,  $a_m(v) = 0$ . Thus the slow equations governing the activity of  $F$  in the silent state are

$$\begin{aligned} 0 &= f(v, w) \\ w' &= -w/\tau_L \\ a'_h &= [1 - a_h]/\tau_{lo}. \end{aligned} \quad (6)$$

Note that while an equation for  $a_h$  is included in (6),  $a_h$  does not actually affect  $F$  in the silent state because  $a_m = 0$ . However, upon leaving the silent state, the value of  $a_h$  affects the  $F$  dynamics. When  $F$  is in the active state,  $a_m(v) = 1$  and the slow equations are

$$\begin{aligned} 0 &= f(v, w) - \bar{g}_a a_h [v - E_K] \\ w' &= [w_\infty(v) - w]/\tau_R \\ a'_h &= -a_h/\tau_{hi}. \end{aligned} \quad (7)$$

There are two sets of fast equations which govern the transition of  $F$  from the silent to the active

state. On the interval  $v_{lk} < v < v_\theta$  the fast equations are

$$\begin{aligned}\dot{v} &= f(v, w) \\ \dot{w} &= 0 \\ \dot{a}_h &= 0,\end{aligned}\tag{8}$$

whereas for  $v_\theta < v$  these equations are

$$\begin{aligned}\dot{v} &= f(v, w) - \bar{g}_a a_h [v - E_K] \\ \dot{w} &= 0 \\ \dot{a}_h &= 0.\end{aligned}\tag{9}$$

As we will show in the Results section, the addition of an  $A$  current in (9) causes the  $v$ -nullcline of  $F$  to have a quintic shape. We refer to this quintic  $v$ -nullcline as  $\mathcal{Q}_o$ . The simplifying assumption that the activation of the  $A$  current is all-or-none restricts this middle branch of  $\mathcal{Q}_o$  to lie on  $v = v_\theta$ . For simplicity of analysis, we will assume that the kinetics of the intrinsic variable  $w$  on the middle branch are much slower than the inactivation of the  $A$  current (in a neighborhood of  $v_\theta$ ,  $\tau_w(v) \gg \tau_{med}$ ). Thus on the middle branch,  $w$  does not change and remains at the value  $w_{lk}$  from which the  $F$  trajectory left the silent state. With this assumption, the equations for  $F$  on the middle branch are

$$\begin{aligned}v' &= 0 \\ w' &= 0 \\ a'_h &= -a_h/\tau_{med}.\end{aligned}\tag{10}$$

## 2.4 The $O$ to $F$ synapse

The synapse from  $O$  to  $F$  is modeled as an inhibitory depressing synapse (Bose et al., 2001; Manor et al., 2003). The synaptic current is incorporated in the model by adding the term  $I_{syn} = \bar{g}_{syn} s [v - E_{syn}]$  to the right side of the  $v$  equations in equations (5-9). The parameters  $\bar{g}_{syn}$  and  $E_{syn}$  are the maximal conductance and reversal potential of the synapse, respectively. To ensure that the synapse is inhibitory, we choose  $E_{syn}$  to be less than  $v_{lk}$ . The variable  $s$  denotes the synaptic efficacy and lies between 0 and 1. The value of  $s$  depends on another variable  $d$  that measures the extent of depression in the inhibitory synapse. The equations governing  $s$  and  $d$  are

$$\begin{aligned}d' &= \begin{cases} (1-d)/\tau_\alpha & v_O < v_{thresh} \\ -d/\tau_\beta & v_O \geq v_{thresh} \end{cases} \\ s' &= \begin{cases} -s/\tau_\kappa & v_O < v_{thresh} \\ (d_0 - s)/(\epsilon\tau_\eta) & v_O \geq v_{thresh} \end{cases}\end{aligned}\tag{11}$$

where  $d_0$  is the value of  $d$  when  $O$  becomes active ( $v_O$  crosses  $v_{thresh}$  with positive slope). Figure 3 shows time traces of variables  $d$  and  $s$  for two cycles of the oscillator neuron  $O$ . When  $O$  becomes active,  $s$  approaches  $d_0$  with time constant  $\epsilon\tau_\eta$ . In the limit as  $\epsilon \rightarrow 0$  this implies that  $s = d_0$

during the entire active state of  $O$ . When  $O$  becomes silent,  $s$  decays with time constant  $\tau_\kappa$ . The parameters  $\tau_\alpha$  and  $\tau_\beta$  are the recovery and depression time constants, respectively. These time constants determine the dependence of  $d$  on the activity of the oscillator  $O$  (Fig. 3).

The value  $d_0$  can be calculated using the periodicity of  $O$ . From equation (11), when  $O$  becomes active,  $d' = -d/\tau_\beta$ . Thus  $d(T_{act}) = d_0 \exp(-T_{act}/\tau_\beta)$ . When  $O$  is silent  $d' = [1 - d]/\tau_\alpha$ . Solving this equation with the condition on  $d(T_{act})$  given above and using the periodicity condition  $d(T_{act} + T_{inact}) = d_0$ , we obtain

$$d_0 = \frac{1 - \exp(-T_{inact}/\tau_\alpha)}{1 - \exp(-T_{inact}/\tau_\alpha) \exp(-T_{act}/\tau_\beta)}.$$

For convenience we keep track of the synaptic conductance  $g_s = \bar{g}_{syn}s$  instead of the synaptic variable  $s$ . Just before  $O$  becomes active,  $g_s$  is at its minimum value denoted by  $g_{min}$ . Just after it becomes active,  $g_s$  is reset to its maximum value denoted by  $g_{peak}$  (see the  $s$  trace in Fig. 3). The value  $g_{peak} = \bar{g}_{syn}d_0$ , which can be rewritten as

$$g_{peak} = \bar{g}_{syn} \frac{1 - \exp(-T_{inact}/\tau_\alpha)}{1 - \exp(-T_{inact}/\tau_\alpha) \exp(-T_{act}/\tau_\beta)}. \quad (12)$$

The above equation shows how the relative strength of the depressing synapse depends on the time constants of recovery and depression, and on  $T_{act}$  and  $T_{inact}$ . Thus in the case where the synapse is depressing, as period changes,  $g_{peak}$  will, in general, change as well. However when we consider cases involving a non-depressing synapse, we let  $d(t) \equiv 1$  and thus  $g_{peak}$  is constant.

## 2.5 The reduced equations

The activity of  $F$  in the presence of synaptic input from  $O$  and an intrinsic  $A$  current is governed by

$$\begin{aligned} \epsilon v' &= f(v, w) - \bar{g}_a a_h a_m [v - E_K] - g_s [v - E_{syn}] \\ w' &= [w_\infty(v) - w]/\tau_w(v) \\ a'_h &= [h_\infty(v) - a_h]/\tau_h(v) \\ a_m &= H(v - v_\theta) \\ d' &= \begin{cases} (1 - d)/\tau_\alpha & v_O < v_{thresh} \\ -d/\tau_\beta & v_O \geq v_{thresh} \end{cases} \\ g'_s &= \begin{cases} -g_s/\tau_\kappa & v_O < v_{thresh} \\ (\bar{g}_{syn}d_0 - g_s)/(\epsilon\tau_\eta) & v_O \geq v_{thresh} \end{cases} \end{aligned} \quad (13)$$

The activity of  $F$  on different branches of the quintic  $v$ -nullcline is governed by reduced equations obtained when setting  $\epsilon = 0$  in equation (13). These are the equations upon which all the analyses

in this work are based. When  $O$  is active (and  $F$  is silent) then

$$\begin{aligned}
0 &= f(v, w) - g_s[v - E_{syn}] \\
w' &= -w/\tau_L \\
a'_h &= [1 - a_h]/\tau_{lo} \\
d' &= -d/\tau_\beta \\
g_s &= g_{peak},
\end{aligned} \tag{14}$$

where  $g_{peak}$  is given by equation (12). When  $O$  and  $F$  are both silent then

$$\begin{aligned}
0 &= f(v, w) - g_s[v - E_{syn}] \\
w' &= -w/\tau_L \\
a'_h &= [1 - a_h]/\tau_{lo} \\
d' &= [1 - d]/\tau_\alpha \\
g'_s &= -g_s/\tau_\kappa.
\end{aligned} \tag{15}$$

When  $O$  is silent and  $F$  is on the middle branch of the quintic  $v$ -nullcline then

$$\begin{aligned}
v' &= 0 \\
w' &= 0 \\
a'_h &= -a_h/\tau_{med} \\
d' &= [1 - d]/\tau_\alpha \\
g'_s &= -g_s/\tau_\kappa.
\end{aligned} \tag{16}$$

Finally, when  $O$  is silent and  $F$  is active then

$$\begin{aligned}
0 &= f(v, w) - g_s[v - E_{syn}] - \bar{g}_a a_h[v - E_K] \\
w' &= [w_\infty(v) - w]/\tau_R \\
a'_h &= -a_h/\tau_{hi} \\
d' &= [1 - d]/\tau_\alpha \\
g'_s &= -g_s/\tau_\kappa.
\end{aligned} \tag{17}$$

### 3 Results

Our general goal is to derive a mathematical expression for the activity phase  $\phi$  of the follower neuron  $F$  in terms of parameters of the depressing synapse and the  $A$  current. The results are divided into three main parts. In the first part, we derive an expression for  $t_f$  (Fig. 1), the time that  $F$  spends in its inhibited or silent state (on the left branch of its  $v$  nullcline). In section (3.1) we show the effect of synaptic inhibition on the  $F$  nullclines. We then describe how depression determines the peak of the synaptic strength at different periods of  $O$ . In section (3.2), we derive equation (18) that describes how  $t_f$  is related to the parameters of the model.

The contribution of the  $A$  current is dealt with in the second part of the results. Here, we derive an expression for  $t_a$  (Fig. 1), the time delay produced by the  $A$  current between the silent (low-voltage) and active (high-voltage) states of  $F$ . This is done by first establishing the effect of the  $A$  current on the  $F$  nullclines in section (3.3). In this section we also provide a necessary condition, equation (22), for the  $A$  current to produce a delay (i.e.,  $t_a > 0$ ). In section (3.4) we use these conditions to derive an estimate (equation (25)) on how large  $t_f$  needs to be in order for  $t_a > 0$ . Assuming equation (25) is satisfied, we then derive an equation (27) that describes how  $t_a$  is related to  $t_f$  and other parameters of the model.

Finally, in section (3.5), the expressions for  $t_f$  and  $t_a$  are used to compute the phase  $\phi$  of  $F$  activity. We examine the dependence of phase on period  $P$  for one specific case where the period is changed by changing only the duration of the silent state of the oscillator ( $T_{inact}$ ). In this section we demonstrate the phase versus period relationships for four cases: no depression and no  $A$  current, no depression with  $A$  current, depression and no  $A$  current, and depression with  $A$  current.

### 3.1 The effect of the $O$ to $F$ synapse on the nullclines of $F$

Inhibition, in general, tends to shift the  $v$  nullcline  $\mathcal{C}_o$  down in the  $v-w$  phase plane and the greater the inhibition (larger  $g_{peak}$ ), the larger the shift in  $\mathcal{C}_o$  (Fig. 4). Inhibition causes the  $F$  trajectory to land on the left branch, as shown in panels A and B of Fig. 4. If synaptic inhibition ( $g_s$ ) does not decay while  $O$  is silent, the trajectory of  $F$  would remain on the cubic nullcline corresponding to  $g_s = g_{peak}$  (the lower nullcline of panels A and B). However, since the strength of inhibition decays with time constant  $\tau_\kappa$  when  $O$  is silent, the trajectory of  $F$  does not stay on any one cubic nullcline; it starts from the nullcline corresponding to  $g_s = g_{peak}$  and moves towards the nullcline  $\mathcal{C}_o$  corresponding to  $g_s = 0$ . This can be seen in the trajectories shown in panels A and B.

The local minimum points of these inhibited cubics form a curve (Fig. 4A and B). The trajectory of  $F$  must reach this curve in order for  $F$  to leave the silent state. We call this curve the jump curve. Note that when the inhibition is weak, the jump curve does not intersect the sigmoidal nullcline  $\mathcal{S}_o$  (Fig. 4A). However, when the inhibition is strong, the jump curve and  $\mathcal{S}_o$  intersect (Fig. 4B). The value of  $g_s$  at which the jump curve intersects  $\mathcal{S}_o$  is denoted  $g_s^*$ .

Inhibition also shifts down the right branches of the cubic nullcline (Fig. 4C). Thus, once  $O$  becomes active again, it causes  $F$  to jump down to the left branch of the cubic with  $g_s = g_{peak}$  and  $w = w_0$  which is smaller than but close to  $\hat{w}$ .

When the synapse is depressing, the strength of inhibition is a function of the period of  $O$  as determined by equation (12). Thus, depending on the period of  $O$ , the inhibitory synapse may be weak, resulting in an  $F$  trajectory as in Fig. 4A, or strong, resulting in an  $F$  trajectory as in Fig. 4B.

### 3.2 The dependence of $t_f$ on the oscillation period and the synaptic and intrinsic parameters

In this section we derive the time delay  $t_f$  between the onset of activity in  $O$  and the onset of activity in  $F$  when  $F$  does not have an  $A$  current ( $\bar{g}_a = 0$ ). This is the time that  $F$  spends on the left branch of the  $v$ -nullcline. Let's assume that  $F$  jumps to the left branch at  $t = 0$ . In order to calculate  $t_f$  we follow the trajectory of  $F$  on the left branch of  $\mathcal{C}_o$  (see Fig. 4). The part of the trajectory is controlled by the dynamics of two independent variables  $g_s$  and  $w$ . This trajectory ends at the “jump curve”, the curve where the left branch of the  $v$  nullcline loses stability in the fast system. The jump curve can be linearly approximated as  $g_s = g_s^* - Mw$  where the parameter  $M$  is a positive constant (Bose et al., 2001). The parameter  $M$  is a proportionality factor that indicates that a jump point with a smaller value of  $w$  corresponds to stronger inhibition (larger  $g_s$ ; see Fig. 4A and B).

At the time ( $t = 0$ ) when  $O$  becomes active and  $F$  jumps to the silent state,  $g_s(0) = g_{peak}$  and  $w(0) = w_0$ . Thus, using this linear relationship for the jump curve and the reduced equations (14-15) we obtain the following implicit equation involving  $t_f$ :

$$g_{peak} \exp(-(t_f - T_{act})^+/\tau_\kappa) + Mw_0 \exp(-t_f/\tau_L) = g_s^*, \quad (18)$$

where  $(t_f - T_{act})^+ = t_f - T_{act}$  if  $t_f > T_{act}$  or 0 if  $t_f < T_{act}$ . Equation (12) for  $g_{peak}$  and equation (18) completely determine the delay  $t_f$ . In the case of a non-depressing synapse,  $g_{peak}$  is constant for all values of  $P$ . Thus, equation (18) implies that  $t_f$  is constant for all  $P$ . In contrast, when the synapse is depressing  $t_f$  may be dependent on  $P$  since  $g_{peak}$  is a function of  $T_{inact}$  and  $T_{act}$ .

When  $g_{peak}$  is either large enough or small enough, equation (18) can be simplified and explicitly solved for  $t_f$ . When  $g_{peak}$  is small enough ( $g_{peak} \ll Mw_0$ ), the first term on the left hand side of equation (18) can be ignored and the equation can be solved for  $t_f$  to obtain

$$t_f = \tau_L \ln \frac{Mw_0}{g_s^*}. \quad (19)$$

The time  $t_f$  in this case is constant with respect to  $P$  and mainly determined by  $\tau_L$  which is an intrinsic time constant of  $F$  governing its evolution in the silent state (Fig. 4A). In contrast, when  $g_{peak}$  is large, the first term on the left hand side equation (18) can dominate the second. This will occur if  $\bar{g}_{syn} > g_s^*$  and  $\tau_\kappa \gg \tau_L$ . Again the equation can be solved for  $t_f$  to obtain

$$t_f = \tau_\kappa \ln \frac{g_{peak}}{g_s^*} + T_{act}. \quad (20)$$

Here the most relevant time constant in determining  $t_f$  is  $\tau_\kappa$ , the time constant of synaptic decay following the active state of  $O$ . In this case (large  $g_{peak}$ ),  $t_f$  is an increasing function of  $g_{peak}$ .

### 3.3 The effect of the $A$ current on the nullclines

Now that we have established the dependence of  $t_f$  on  $P$  in the presence of depression, we will describe how the existence of an outward  $A$  current in the follower neuron  $F$  can affect this relationship. We shall do this in two steps. First, we will establish the conditions that must hold for the  $A$  current to produce a delay in the activity of  $F$ . This additional delay would occur in the transition of  $F$  from the silent state (the left branch of the  $v$  nullcline) to the active state (the right branch of the  $v$  nullcline). Second, we will measure the additional delay caused by the  $A$  current once these conditions are satisfied.

We will first discuss the effect of the  $A$  current on the dynamics of  $F$  in the absence of the inhibitory synapse. The effect of the  $A$  current is to change the shape of the  $v$  nullcline. Specifically, the additional term  $\bar{g}_a a_h [v - E_K]$  in equation (9) causes the part of  $\mathcal{C}_o$  to the right of  $v = v_\theta$  (where the  $A$  current activates) to shift down in the phase plane. The larger the magnitude of  $I_A$ , the larger the shift (Fig. 5). Thus the  $v$ -nullcline in the presence of  $I_A$ , as given by equations (8-9) is quintic shaped. We denote this quintic nullcline as  $\mathcal{Q}_o$ . The middle branch of  $\mathcal{Q}_o$  lies on the vertical line  $v = v_\theta$ . The local maximum along the middle branch of  $\mathcal{Q}_o$  occurs at  $w = w_\theta$  where  $w_\theta$  satisfies  $f(v_\theta, w_\theta) = 0$ . The minimum value depends on how big  $a_h$  becomes while  $F$  is in the silent state. Since  $F$  leaves the silent state when  $t = t_f$ , the size of the  $A$  current at this instant is determined by  $a_h(t_f) = [1 - \exp(-t_f/\tau_{lo})]$ . Therefore the minimum  $w$  value along the middle branch, denoted  $w_{min}$ , satisfies

$$f(v_\theta, w_{min}) - \bar{g}_a a_h(t_f)[v_\theta - E_K] = 0.$$

In the absence of synaptic input,  $F$  leaves the silent state from  $w_{lk}$ . Let us denote by  $a_h^*$  the value of  $a_h$  which satisfies

$$f(v_\theta, w_{lk}) - \bar{g}_a a_h^*[v_\theta - E_K] = 0.$$

By solving for  $a_h^*$ , we obtain

$$a_h^* = \frac{f(v_\theta, w_{lk})}{\bar{g}_a [v_\theta - E_K]}. \quad (21)$$

This is the value of  $a_h$  at which the minimum along the middle branch matches the minimum along the left branch of the quintic. Further observe that if  $w_{min} < w_{lk}$ , then the trajectory of  $F$  lands on the middle branch. Assuming  $\partial f/\partial w < 0$  beneath  $\mathcal{C}_o$ , a simple condition ensuring that the trajectory of  $F$  lands on the middle branch is

$$a_h(t_f) > a_h^*. \quad (22)$$

Thus, in order for  $F$  to land on the middle branch of  $\mathcal{Q}_o$ , thereby allowing the  $A$  current to delay the activity of  $F$ , two conditions must be met. First, the maximal conductance of the current ( $\bar{g}_a$ ) needs to be large enough so that the right-hand side of (21) is less than 1. Second,  $F$  needs to spend enough time on the left branch for the  $A$  current to sufficiently recover from inactivation, so that equation (22) is satisfied.

### 3.4 Determining $t_a$

We now discuss how the  $A$  current and the inhibitory synapse interact to affect the activity of  $F$ . Although these two processes are independent, their interaction determines whether or not the  $F$  trajectory lands on the middle branch of the quintic and, if so, how long it stays there. Specifically, while  $F$  is in its silent state (between  $t = 0$  and  $t = t_f$ ) two processes evolve that determine  $t_a$ . First,  $g_s$  decays causing the  $w$ -value, denoted  $w_{lk}(g_s(t_f))$ , from which  $F$  leaves the silent state to be dependent on  $g_s$  (see Fig 6A). From equation (18) for the jump curve, we find that  $w_{lk}(g_s(t_f))$  satisfies  $g_s(t_f) + Mw_{lk}(g_s(t_f)) = g_s^*$ . Second,  $a_h$  grows, causing the middle branch of the  $v$ -nullcline to move down. As seen in Fig. 6A, if at the time  $t = t_f$  (when  $F$  leaves its silent state), the minimum point of the middle branch is below  $w = w_{lk}(g_s(t_f))$  (denoted by the horizontal dotted line), the  $F$  trajectory lands on the middle branch. As in the derivation of  $a_h^*$  in equation (21), the value of  $a_h$  (now referred to as  $a_h^*(t_f, g_s)$ ) for which the minimum value of the left branch of the inhibited  $v$ -nullcline matches the minimum value of its middle branch can be calculated analytically. From equation (13), the middle branch of the  $v$  nullcline is given by

$$f(v_\theta, w) - \bar{g}_a a_h [v_\theta - E_K] - g_s [v_\theta - E_{syn}] = 0. \quad (23)$$

Thus,  $a_h^*(t_f, g_s)$  satisfies

$$a_h^*(t_f, g_s) = \frac{f(v_\theta, w_{lk}(g_s(t_f))) - g_s(t_f)[v_\theta - E_{syn}]}{\bar{g}_a [v_\theta - E_K]}. \quad (24)$$

Note that when  $g_s = 0$ , then (24) reduces to (21). Thus, in general, the necessary condition for  $F$  to land on the middle branch of the quintic  $v$ -nullcline is that  $a_h(t_f) > a_h^*(t_f, g_s)$ . Substituting  $a_h(t_f) = 1 - \exp(-t_f/\tau_{lo})$  and solving for  $t_f$ , we can derive an estimate on how large  $t_f$  needs to be in order for  $t_a > 0$ . Namely, if

$$t_f > \tau_{lo} \ln \frac{1}{1 - a_h^*(t_f, g_s)}, \quad (25)$$

then  $F$  will land on the middle branch of  $\mathcal{Q}_o$  and  $t_a > 0$ . Otherwise,  $a_h$  is too small, causing the trajectory of  $F$  to jump directly to the right branch and thus  $t_a = 0$ . The inequality (25) implicitly gives information about the rate at which  $I_A$  deactivates relative to the rate at which  $I_{syn}$  decays in the silent state. The right-hand side of (25) is most strongly affected by  $\tau_{lo}$ , the time constant at which  $I_A$  grows when  $F$  is silent. The left-hand side is most strongly affected (for large  $g_{peak}$ ) by  $\tau_\kappa$ , the time constant controlling the decay of synaptic inhibition  $I_{syn}$  (as seen from equation (20)). Thus, if  $\tau_{lo}$  is large, then inhibition must decay slowly to allow  $I_A$  to play a role in determining  $t_a$ . Indeed, if (25) is not satisfied, then  $t_a = 0$ .

When (25) is satisfied, we can derive an expression for  $t_a$ . On the middle branch,  $a_h' = -a_h/\tau_{med}$ . Thus

$$a_h(t) = [1 - e^{-t_f/\tau_{lo}}]e^{-(t-t_f)/\tau_{med}}. \quad (26)$$

On the middle branch  $w = w_{lk}(g_s(t_f))$ . During the time interval  $t_a$ , the conductances  $\bar{g}_a a_h$  and  $g_s$  decay until the minimum on the middle branch of the quintic  $v$ -nullcline passes through the value

$w = w_{lk}(g_s(t_f))$  (Fig. 6B). At this moment  $F$  leaves the middle branch and makes a fast excursion to the active state. Thus, the value of  $t_a$  can be calculated from equation (23) for the middle branch of the  $v$ -nullcline from the following equation

$$f(v_\theta, w_{lk}(g_s(t_f))) = \bar{g}_a a_h(t_f) e^{-t_a/\tau_{med}} [v_\theta - E_K] + g_s(t_f) e^{-t_a/\tau_\kappa} [v_\theta - E_{syn}]. \quad (27)$$

The right-hand side of (27) is a monotone decreasing function of  $t_a$ , while the left-hand side is independent of  $t_a$ . Thus (by the Implicit Function Theorem), for each value of  $t_f$ , there is a unique value of  $t_a$  which satisfies (27). This transcendental equation implicitly determines the value of  $t_a$ . If the inactivation of the  $A$  current is much slower than the decay of the inhibitory synapse ( $\tau_{med} \gg \tau_\kappa$ ), equation (27) can be simplified by ignoring the second term on the right-hand side, and we obtain

$$t_a = \tau_{med} \ln \frac{\bar{g}_a [1 - e^{-t_f/\tau_o}] [v_\theta - E_K]}{f(v_\theta, w_{lk}(g_s(t_f)))}. \quad (28)$$

Equation (28) shows that if  $F$  spends a longer time ( $t_f$ ) in its silent state (and if (25) is satisfied), the delay ( $t_a$ ) produced by the  $A$  current becomes longer.

We have now calculated the times that the  $F$  neuron trajectory spends both on the left branch and on the middle branch of the  $v$ -nullcline. These results are summarized in Fig. 7 by showing a full cycle of the  $F$  neuron trajectory. In Fig. 7A, we show this trajectory in the  $v - w$  phase plane with key transition points marked from the beginning the  $O$  active state to the end of the cycle. Fig. 7B shows the same transition points on the voltage trace of  $F$ . In this cycle, the slow equations determine the time intervals from 2 to 3 ( $t_f$ ), from 4 to 5 ( $t_a$ ) and from 6 to 7 ( $P - t_f - t_a$ ). The transitions from 1 to 2, 3 to 4 and 7 to 1 are determined by the fast equations and in our analysis are instantaneous.

### 3.5 The activity phase as function of period

In this section we use the analytical formulas derived for  $t_f$  and  $t_a$  in the previous sections to calculate the activity phase ( $\phi = (t_f + t_a)/P$ ) of  $F$  as function of  $P$ . We compare 4 cases, defined by the presence or absence of synaptic depression and of  $I_A$  in  $F$ . These results are shown in Fig. 9. In making this figure, the period is treated as a parameter and modified by changing  $T_{inact}$  while keeping  $T_{act}$  constant.

Increasing  $T_{inact}$  allows for more recovery from depression and strengthens the synapse, i.e.,  $g_{peak}$  in equation (12) becomes larger. A graph of equation (12) is shown in Fig. 8 by plotting  $g_{peak}$  versus  $P$ . For small values of  $P$ ,  $g_{peak}$  is small, which corresponds to a weak synapse. In this case,  $T_{inact}$  is too small to allow the synapse to sufficiently recover from depression. Note that for  $T_{inact}$  large enough, the synapse maximally recovers from depression ( $g_{peak}$  asymptotically approaches  $\bar{g}_{syn}$  as  $P \rightarrow \infty$ ). The derivative of  $g_{peak}$  with respect to  $P$ , although positive, exponentially decays to 0 as  $P$  increases (Fig. 8). We will use this fact later to calculate the phase of  $F$  activity.

Consider first the cases where the synapse from  $O$  to  $F$  is non-depressing. In these cases,  $t_f$  is fixed. If  $I_A = 0$  or small,  $t_a = 0$  and therefore the phase  $\phi$  is a monotonic decreasing function of

$P$  (Fig. 9A). If  $I_A$  is sufficiently strong,  $t_a > 0$  but is fixed and independent of  $P$ , because  $t_f$  is fixed. Thus the phase curve is again a monotonically decreasing function of  $P$ , albeit shifted up with respect to the case where  $I_A$  is small (Fig. 9B).

In the other two cases, the synapse from  $O$  to  $F$  is depressing, and therefore the strength of the synapse depends on the extent of depression and recovery from it. These, in turn, depend on the durations of the active and silent states (and thus period) of  $O$ . When  $I_A$  is non-existent or small,  $t_f$  is the only delay between the activity of  $O$  and  $F$ . In this case, with appropriate choice of parameters, the dependence of  $\phi$  on  $P$  can be cubic (Fig. 9C).

We can make use of the relationship between  $t_f$  and  $P$  (established by equations (19) and (20)) to understand the dependence of phase  $\phi$  on  $P$  when  $I_A$  is absent ( $t_a = 0$  and  $\phi = t_f/P$ ). When  $P$  is small  $g_{peak}$  is small, and equation (19) implies that  $t_f$  is constant. Thus,  $\phi$  decreases with  $P$ . When  $P$  is large enough, equation (20) implies that  $t_f$  is an increasing function of  $P$ . This follows from the fact that  $g_{peak}$  is an increasing function of  $T_{inact}$  and therefore of  $P$  (equation (12) and Fig. 8). In this case, the dependence of  $\phi$  on  $P$  is more complex. From equation (20) we see that

$$\phi = \frac{\tau_\kappa}{P} \ln \frac{g_{peak}}{g_s^*} + \frac{T_{act}}{P}.$$

Whether  $\phi$  is increasing or decreasing depends on the sign of the derivative  $d\phi/dP$  given by

$$\frac{d\phi}{dP} = \frac{\tau_\kappa}{P} \left[ \frac{dg_{peak}/dP}{g_{peak}} - \frac{1}{P} \ln \frac{g_{peak}}{g_s^*} - \frac{T_{act}}{P\tau_\kappa} \right].$$

Note that at the value of  $P$  ( $= P^*$ ) for which  $g_{peak} = g_s^*$  (Fig. 8), the expression  $\frac{dg_{peak}/dP}{g_{peak}} - \frac{T_{act}}{P\tau_\kappa}$  is positive if either  $\tau_\kappa$  is large enough or if  $T_{act}$  is small enough. The former condition means that the synapse decays slowly, while the latter means that the synapse has a very small amount of time to depress in each cycle. In these cases,  $d\phi/dP > 0$  and thus, for  $P$  values close to  $P^*$ ,  $\phi$  increases with  $P$ .

Next consider the case where the cycle period is very large ( $P \rightarrow \infty$ ). Then  $g_{peak} \rightarrow \bar{g}_{syn}$  and  $dg_{peak}/dP \rightarrow 0$  (Fig. 8). Since  $dg_{peak}/dP \rightarrow 0$  exponentially fast (in particular, faster than  $1/P$ ),  $d\phi/dP < 0$  and thus  $\phi$  decreases for large values of  $P$ . Thus, for the appropriate choice of parameters, as  $P$  increases from very small to very large values,  $\phi$  is initially decreasing, then increasing and finally decreasing again (Fig. 9C).

Finally, when  $I_A$  is sufficiently strong, the delay between the onsets of activities in  $O$  and  $F$  is  $t_f + t_a$ , where  $t_a$  is a monotonic increasing function of  $t_f$ . This synergistic interaction give rise to the complex relationship shown in (Fig. 9D). In this case, the phase curve has two local minima and two local maxima and is qualitatively ‘‘quintic’’ shaped. The second set of local extrema is due solely to contribution of the  $A$  current. Let  $P_1 < P_2$  denote the values of period at the two local minima. In this figure, we have chosen  $\tau_{l_o}$  large enough so that  $I_A$  does not become relevant until  $P > P_2$ . In this range of periods,  $t_a$  is primarily determined by the parameter  $\tau_{med}$ , the inactivation time constant of the  $A$  current on the middle branch of  $\mathcal{Q}_o$ . This time constant is independent

of both  $\tau_L$  (the intrinsic time constant of  $F$  on the left branch) and  $\tau_\kappa$  (the synaptic decay time constant) which, respectively, determined phase in the ranges  $P < P_1$  and  $P_1 < P < P_2$ . Thus by choosing  $\tau_{med}$  to be sufficiently large and  $\tau_{lo}$  satisfying (25), a second set of local extrema was obtained.

The addition of  $I_A$  into the description of  $F$  provides the network with another way to determine phase. There are now four important and independent time constants which determine phase,  $\tau_L$ ,  $\tau_\kappa$ ,  $\tau_{lo}$  and  $\tau_{med}$ . By choosing them appropriately, the phase curve can have 0 (monotonically decreasing), 2 (cubic shaped) or 4 (quintic shaped) local extrema. The analysis leading to equations (18) and (27) shows which of these (and other) parameters control the locations of these extrema and the  $\phi$  values at these points. For example, when  $\tau_\kappa$  is small relative to  $\tau_L$ ,  $\phi$  is determined solely by  $\tau_L$  or  $\tau_{med}$  and is monotonically decreasing. When  $\tau_\kappa$  is large relative to  $\tau_L$ , but  $\tau_{med}$  is small or  $\tau_{lo}$  is large relative to  $\tau_\kappa$ , the phase curve is cubic. Finally, when  $\tau_\kappa$  and  $\tau_{med}$  are large relative to  $\tau_L$  and  $\tau_{lo}$  is not so large relative to  $\tau_\kappa$  and satisfies (25), the phase curve is quintic shaped.

## 4 Discussion

Many behaviors are mediated by oscillatory networks and require proper phase relationships among the neurons involved. In olfactory processing, for example, different odors are encoded by patterns of phase of different neurons with respect to the field oscillation (Laurent et al., 1996). Hippocampal place cells use the phase of activity to encode for the location of the animal. The firing phase of the neuron with respect to the field theta rhythm advances as the animal moves through the neuron's place field (O'Keefe and Recce, 1993). Thus the activity phase of neurons need not be locked to the field oscillation but may change with a consistent pattern. In many central pattern generators (CPGs), the phase difference between different members of the CPG is often kept constant despite wide changes in frequency. For example, in chains of coupled oscillators, the phase difference between adjacent oscillators remains constant independent of frequency (Skinner and Mulloney, 1998). In the crustacean pyloric circuit, the tri-phasic pattern of activity is maintained despite large changes in frequency (Hooper, 1997a). This robustness emerges from the ability of pairs of neurons to maintain fixed phase when frequency changes (Hooper, 1997b).

A common question in all these systems is how the activity phase of neurons is controlled. We addressed this question in an inhibitory oscillator-follower network. An inhibitory synapse can trigger the activation of a particular set of currents, which can subsequently advance or delay the activity of the follower. An important class of such currents are the transient potassium currents, also known as  $A$  currents. One property of the  $A$  current is that it is usually inactivated at rest. Following hyperpolarization, the  $A$  current is deinactivated and, upon repolarization, can delay activity (Harris-Warrick et al., 1995; Hess and Manira, 2001; Hsiao and Chandler, 1995).

In this work, we analyzed a simplified model network involving an inhibitory depressing synapse between an oscillator  $O$  and a follower  $F$  neuron that has an  $A$  current. In our model, we divided the latency between  $O$  and  $F$  into two distinct components, one incorporating the effects of synaptic

inhibition of  $F$  ( $t_f$ ) and the other incorporating the effects of the  $A$  current ( $t_a$ ). Using the derived mathematical expressions for  $t_f$  and  $t_a$ , we found that the  $A$  current delays the activity of  $F$  only when  $t_f$  is long enough, because in this case,  $t_a$  is an increasing function of  $t_f$ .

The mathematical expressions for  $t_a$  and  $t_f$  can be used to calculate the phase of  $F$  as a function of period. We have shown this relationship for the case where the period is changed by changing only the duration of the silent state of the oscillator. In this case, a non-depressing synapse produces a constant  $t_f$  and  $t_a$ , resulting in a monotonically decreasing phase curve. However, when the synapse is depressing, its strength changes with period. As a result,  $t_f$  and consequently  $t_a$  are dependent on period as well. With an appropriate choice of parameters the relationship between phase and period can be monotonic, cubic or quintic shaped. Thus, with a depressing synapse, the choice of model parameters allows different mechanisms to control the phase in different period ranges. For example, at small periods, when the synapse is weak, phase is determined by the intrinsic dynamics of  $F$  in its silent state (determined by  $\tau_L$ ). At intermediate periods, the synapse recovers from depression and phase is mostly determined by the decay time constant ( $\tau_\kappa$ ) of the synapse. At larger periods, the synapse is almost maximally recovered from depression. In this range, the  $A$  current dynamics ( $\tau_{med}$ ) determine phase. Note that the period-dependent contribution of the  $A$  current is a direct consequence of the period-dependent recovery of the inhibitory synapse from depression.

## 4.1 Implications of simplifying assumptions

To facilitate the derivation of an analytical expression for  $t_a$ , we made several simplifying assumptions on the dynamics of the  $A$  current. First, we assumed that the steady-state inactivation curve is a step function. The consequence of making this assumption is that the deinactivation of the  $A$  current is only dependent on time. However, experimental measurements of the dynamics of the  $A$  current show that the deinactivation of the  $A$  current can both be a function of voltage and time (Storm, 1990; Thompson, 1977). In contrast to our simplified case, if the deinactivation of the  $A$  current is voltage dependent,  $a_h$  will be affected by the level of hyperpolarization. In this case, a larger hyperpolarization would lead to a larger  $a_h$ , and thus a potentially larger contribution of the  $A$  current.

We also assumed that the activation curve of the  $A$  current is a step function. If it is voltage dependent, the middle branch of the  $v$ -nullcline is no longer vertical but would have negative slope and span a range of voltages. Hence, when the  $A$  current is activated, the voltage would gradually increase, as indeed is observed in experiments (Fig. 1). A voltage dependent activation curve would also have subtle effects on the phase curve. First, it would increase the minimum value of  $t_f$  necessary for  $t_a$  to be nonzero since a stronger  $A$  current would now be necessary for the minimum value along the middle branch to lie below the  $w$  value at which the trajectory leaves the silent state. Secondly, it would shift the phase curve down since the inactivation variable  $a_h$  would not need to decay as much as in the voltage independent case. Thus  $t_a$  would be smaller.

The activation of the  $A$  current was taken to be instantaneous. Relaxing this condition would

have the same qualitative effects as making the activation curve voltage dependent. We have also made the assumption that the  $A$  current inactivates on the middle branch at a faster rate than the evolution of the recovery variable  $w$ . In Hodgkin-Huxley type models, the recovery variable typically evolves very slowly at intermediate voltage values, consistent with our assumption. Removing this condition however, would shift the phase curve up as  $t_a$  would be larger in this case. Note that any other kind of simplifying assumption on the evolution of  $w$  can be used to do the same type of analysis on the middle branch. Finally, we have assumed that activation and inactivation of the  $A$  current occur between the left and right branches of the  $v$ -nullcline. If instead, we assume that these occur on the left branch, then the  $A$  current will have less time to deinactivate before it is activated. This would make the phase smaller at each period.

We also mentioned that the dynamics of  $F$  could be described using Morris-Lecar type equations, although we never explicitly used such equations. The important aspects of the model neuron that are needed for the type of analysis we conducted are that the follower neuron have a high-voltage fixed point and a clearly identifiable recovery process.

Note that all these simplifying assumptions were made merely to make the calculations easier and explicit. Removing any or all of them does not qualitatively change the results that when the synapse is depressing, the phase can be determined by different parameters in different ranges of period.

## 4.2 Different types of oscillators

The derivation of the times  $t_f$  and  $t_a$  hold for any value of  $T_{inact}$  and  $T_{act}$ . Thus, the phase of the follower neuron can be calculated once  $T_{inact}$  and  $T_{act}$  are known. We used this fact to explore how phase changes as a function of period in the special case where period was changed by holding  $T_{act}$  fixed and changing  $T_{inact}$  (Fig. 9). In general, the phase versus period relationship can be obtained when the values of  $T_{inact}$  and  $T_{act}$  are known for any period. The qualitative relationship shown in (Fig. 9) will hold in any case where  $g_{peak}$  is an increasing function of period as in Fig. 8 (for example, when both  $T_{inact}$  and  $T_{act}$  increase but the duty cycle  $T_{act}/P$  remains constant).

Manor et al. (2003) studied how the phase changed as a function of period in three different cases: fixed  $T_{act}$ , fixed  $T_{inact}$  and fixed duty cycle. In the present work, we do not need to make this distinction since we have given equations that can be used to compute the phase-period relationship for any value of  $T_{inact}$  and  $T_{act}$ . In particular, the results numerically computed in Manor et al. (2003) could be analytically computed using equations involving  $t_f$ .

An important aspect that we have not explicitly considered is the issue of feedback from the follower to the oscillator. Although our analysis does not determine how feedback affects the oscillator, once the feedback network has reached steady state, the phase of the follower cell can still be determined using our mathematical expressions. It would be interesting to understand how different types of feedback affect  $T_{act}$  and  $T_{inact}$ , and consequently phase.

### 4.3 Other types of currents

In the current study we chose to focus on the effects of one type of intrinsic current in  $F$ . Other types of ionic currents could contribute to the activity phase of  $F$  as well. The present work provides a framework to study how other such currents may influence phase. We here mention a few examples.

A hyperpolarization activated inward ( $h$ ) current may be activated by an inhibitory input and act to advance the activity of  $F$ . Since this current is activated at low voltages, its main effect is to decrease  $t_f$ . To derive a mathematical expression for  $t_f$ , the relationship between three variables,  $w$ ,  $g_s$  and the activation of the  $h$  current, would need to be established on the left branch of the  $v$ -nullcline. The existence of an  $h$  current could also change the influence of the  $A$  current on phase since  $t_a$  depends on  $t_f$ .

It is intuitively clear that the  $h$  and  $A$  currents can have opposing effects on phase. However, this does not mean that these two effects cancel out, since it is possible that their primary influences occur in different ranges of periods. For example, if the time constant of activation of the  $h$  current is significantly larger than the time constant of inactivation of the  $A$  current, the  $h$  current will advance the phase of  $F$  at much larger periods than the  $A$  current delayed it. Thus the  $h$  current could be used to control the phase in a distinct range of periods, e.g.  $P > P_2$  in Fig. 9.

Another example of an ionic current that, in conjunction with synaptic inhibition, can influence phase is a low-threshold calcium ( $T$ ) current. As with the  $A$  current,  $T$  currents are transient and deinactivate upon hyperpolarization. In contrast to the  $A$  current, the inward  $T$  current advances the activity of  $F$ . In this regard the  $T$  current may act like the  $h$  current to reduce  $t_f$ . However, the  $T$  current activates in a different range of voltages, has faster kinetics than the  $h$  current and, most importantly, is a regenerative current. As such, the  $T$  current could have a significant effect in accelerating the activity of a biological neuron. In our reduced model, such a  $T$  current would have little effect by itself since the transition from the left to right branches of the  $v$ -nullcline is instantaneous. However, if  $F$  has an  $A$  current, the  $T$  current can decrease the delay  $t_a$  and thus advance the activity phase.

## 5 Appendix

We used MATLAB to numerically solve for  $t_f$ ,  $t_a$  and  $\phi$ . The equations we solved were

$$c_1 g_{peak} \exp(-(t_f - T_{act})/\tau_\kappa) + c_2 \exp(-t_f/\tau_L) = c_3. \quad (29)$$

$$g_{peak} = \bar{g}_{syn} \frac{1 - \exp(-T_{inact}/\tau_\alpha)}{1 - \exp(-T_{inact}/\tau_\alpha) \exp(-T_{act}/\tau_\beta)}. \quad (30)$$

The value of  $t_a$  was obtained from

$$r_1 \bar{g}_a (1 - \exp(-t_f/\tau_{lo})) \exp(-t_a/\tau_{med}) + r_2 g_{peak} \exp(-(t_f - T_{act})/\tau_\kappa) \exp(-t_a/\tau_\kappa) = r_3. \quad (31)$$

when  $1 - e^{-t_f/\tau_o} < c_4/\bar{g}_a$  and was 0 otherwise.

$$\phi = \frac{t_f + t_a}{T_{inact} + T_{act}} \quad (32)$$

We used the following set of parameters  $T_{act} = 5$ ,  $\tau_\kappa = 125$ ,  $\tau_L = 15$ ,  $\tau_\alpha = 400$ ,  $\tau_\beta = 5$ ,  $\tau_{lo} = 465$ ,  $\tau_{med} = 1200$ ,  $\bar{g}_{syn} = 4.0$ ,  $\bar{g}_a = 3.5$ ,  $c_1 = 4 \exp(T_{act}/\tau_\kappa)$ ,  $c_2 = 4.6$ ,  $c_3 = 3$ ,  $c_4 = 1.0$ ,  $r_1 = 5.0$ ,  $r_2 = 0.1$  and  $r_3 = 5.0$ . The term  $c_2$  represents  $M\hat{w}(g_{min})$  and for simplicity we have assumed that  $\hat{w}(g_{min})$  is constant. The terms  $c_3 = g_s^*$ ,  $c_4 = a_h^*(t_f, g_s)$  where we have assumed the latter is constant. For cases where the synapse was non-depressing, (9A and B), we used  $\bar{g}_a = 2.35$ .

## Acknowledgments

This work was supported in part by NSF DMS-0315862 (AB), ISF 314/99-1 (YM), BSF 2001-039 (YM, FN) and NIMH 60605-01 (FN).

## References

- Ahissar, E., R. Sosnik, and S. Haidarliu (2000). Transformation from temporal to rate coding in a somatosensory thalamocortical pathway. *Nature* 406, 302–306.
- Bartos, M., Y. Manor, F. Nadim, , and M. Marder, E. Nussbaum (1999). Coordination of fast and slow rhythmic neuronal circuits. *J. Neurosci.* 19, 2247–2256.
- Bose, A., Y. Manor, and F. Nadim (2001). Bistable oscillations arising from synaptic depression. *SIAM J. Appl. Math.* 62, 706–727.
- DiCaprio, R., G. Jordan, and T. Hampton (1997). Maintenance of motor pattern phase relationships in the ventilatory system of the crab. *J. Exp. Biol.* 200, 963–974.
- Harris-Warrick, R., L. Coniglio, N. Barazangi, J. Guckenheimer, and S. Gueron (1995). Dopamine modulation of transient potassium current evokes phase shifts in a central pattern generator network. *J. Neurosci.* 15, 342–358.
- Hess, D. and A. Manira (2001). Characterization of a high-voltage-activated ia current with a role in spike timing and locomotor pattern generation. *Proc. Nat. Acad. Sci.* 98(9), 5276–5281.
- Hooper, S. L. (1997a). Phase maintenance in the pyloric pattern of the lobster (*panulirus interruptus*) stomatogastric ganglion. *J. Comput. Neurosci.* 4, 191–205.
- Hooper, S. L. (1997b). The pyloric pattern of the lobster (*panulirus interruptus*) stomatogastric ganglion comprises two phase-maintaining subsets. *J. Comput. Neurosci.* 4, 207–219.
- Hsiao, C. and S. Chandler (1995). Characteristics of a fast transient outward current in guinea pig trigeminal motoneurons. *Brain Res* 695, 217–26.
- Laurent, G., M. Wehr, and H. Davidowitz (1996). Temporal representations of odors in an olfactory network. *J. Neurosci.* 16, 3837–3847.
- Manor, Y., A. Bose, V. Booth, and F. Nadim (2003). The contribution of synaptic depression to phase maintenance in a model rhythmic network. *J. Neurophysiol.* 90, 3513–3528.
- Marder, E. and R. Calabrese (1996). Principles of rhythmic motor pattern generation. *Physiol. Rev.* 76, 687–717.
- Mishchenko, E. F. and N. K. Rozov (1980). *Differential Equations with Small Parameters and Relaxation Oscillators*. New York: Plenum Press.
- O’Keefe, J. and M. L. Recce (1993). Phase relationship between hippocampal place units and the EEG theta rhythm. *Hippocampus* 3, 317–330.

- Pearson, K. and J. Iles (1970). Discharge patterns of coxal levator and depressor motoneurons of the cockroach, *periplaneta americana*. *J. Exp. Biol.* 52, 139–165.
- Rinzel, J. and G. Ermentrout (1997). In C. Koch and I. Segev (Eds.), *Methods in neuronal modeling: from synapses to networks*, Cambridge, MA, pp. 135–170. MIT Press.
- Skinner, F. and B. Mulloney (1998). Intersegmental coordination of limb movements during locomotion: mathematical models predict circuits that drive swimmeret beating. *J. Neurosci.* 18, 3831–3842.
- Storm, J. (1990). Potassium currents in hippocampal pyramidal cells. *Prog Brain Res* 83, 161–187.
- Thompson, S. (1977). Three pharmacologically distinct potassium channels in molluscan neurones. *J Physiol* 265, 465–488.

## Figure Legends

Figure 1: Approximation of the biological voltage trace. The top voltage trace shows an experimental recording from a crab pyloric PY neuron in response to periodic injection of negative current. We approximate this trace by the smooth middle trace. The bottom trace shows a square wave pulse, representing the oscillator. Important time lengths and timing relationships are also indicated.

Figure 2: A. The  $v - w$  phase plane. The  $v$ -nullcline  $\mathcal{C}_o$  and the  $w$ -nullcline  $\mathcal{S}_o$  intersect uniquely at  $(\hat{v}, \hat{w})$ . A portion of the trajectory is superimposed on the phase plane. It consists of three main parts: slow evolution along the left and right branches of  $\mathcal{C}_o$  and fast evolution between these branches. The transition from the right to left branch is not shown. B. The corresponding voltage trace of  $F$  is shown.

Figure 3: Dynamics of the synaptic ( $s$ ) and the depression ( $d$ ) variables are shown. In the lower trace, the voltage of the oscillator is shown. When the oscillator is active,  $d$  depresses with time constant  $\tau_\beta$  while  $s$  is constant. When the oscillator is inactive,  $d$  recovers with time constant  $\tau_\alpha$ , while  $s$  decays with time constant  $\tau_\kappa$ . The variable  $s$  is reset to  $d$  whenever  $O$  becomes active.

Figure 4: Effect of inhibition on the  $v$ -nullcline. In panels A and B, the local minima of the cubics forms a curve, called the jump curve. A. When inhibition is weak, the time constant of  $w$  ( $\tau_L$ ) is the primary determinant of how much time  $t_f$   $F$  spends in the silent state before reaching the jump curve. B. When inhibition is strong, the time constant of decay of the synapse ( $\tau_\kappa$ ) primarily determines this time. The dashed cubic corresponds to  $g_s = g_s^*$  at which the cubic is tangent to  $\mathcal{S}_o$  on the left branches C. The trajectory of  $F$  never reaches the fixed point  $(\hat{v}, \hat{w})$ , but leaves the right branches due to inhibition while near this fixed point.

Figure 5: The frequency-dependent effect of the  $A$  current on the  $v$ -nullcline. The  $A$  current only affects the  $v$ -nullcline when  $v \geq v_\theta$ . The middle branch of any quintic shaped nullcline lies on  $v = v_\theta$ . The one with  $a_h = a_h^*$  has  $w = w_{lk}$  as its minimum value. The right side of the nullclines moves up as  $a_h$  decreases.

Figure 6: Dynamics before, during and after reaching the middle branch of the  $v$ -nullcline. A. The trajectory of  $F$  lands on the middle branch only when the minimum  $w$  value along the middle branch is less than  $w = w_{lk}(g_s(t_f))$ , the minimum  $w$  value at which  $F$  leaves the silent state (dotted line). B. The trajectory of  $F$  stays on the middle branch until the minimum  $w$  value along the middle branch equals  $w = w_{lk}(g_s(t_f))$ .

Figure 7: Nullclines and trajectory for a full cycle of  $F$ . A. The various panels, from left to right, summarize the behavior of  $F$ 's trajectory in the  $v - w$  phase plane. The numbers in each picture corresponding to specific points as labeled in the lower panel. B. The voltage trace of  $F$  in which relevant points from panel A are shown.

Figure 8: The peak synaptic conductance ( $g_{peak}$ ) and its derivative ( $g'_{peak}$ ) as a function of period. The plots were obtained by keeping  $T_{act}$  fixed and varying only  $T_{inact}$ . The value  $P^*$  is the period at which  $g_{peak} = g_s^*$ .

Figure 9: A-D. Plots of the phase curves versus period in four conditions (each case is represented by a bold trace, other cases are plotted in gray). A, B. The synapse is non-depressing, in the absence and presence of an  $A$  current in  $F$ . C, D. The synapse is depressing, in the absence and presence of an  $A$  current in  $F$ . In D, the periods  $P_1$  and  $P_2$  indicate the local minima of the phase curve (see text).

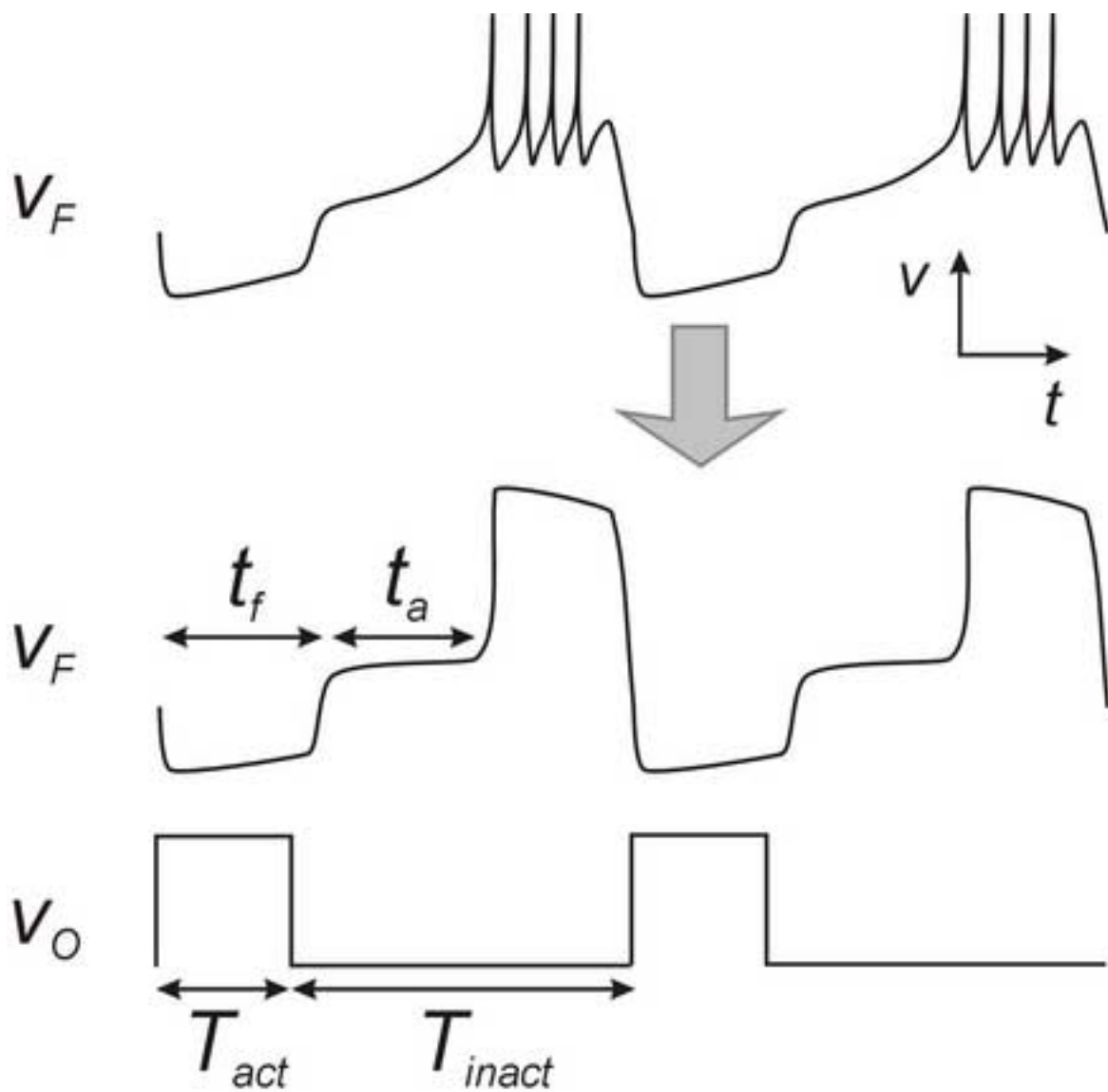


Figure 1

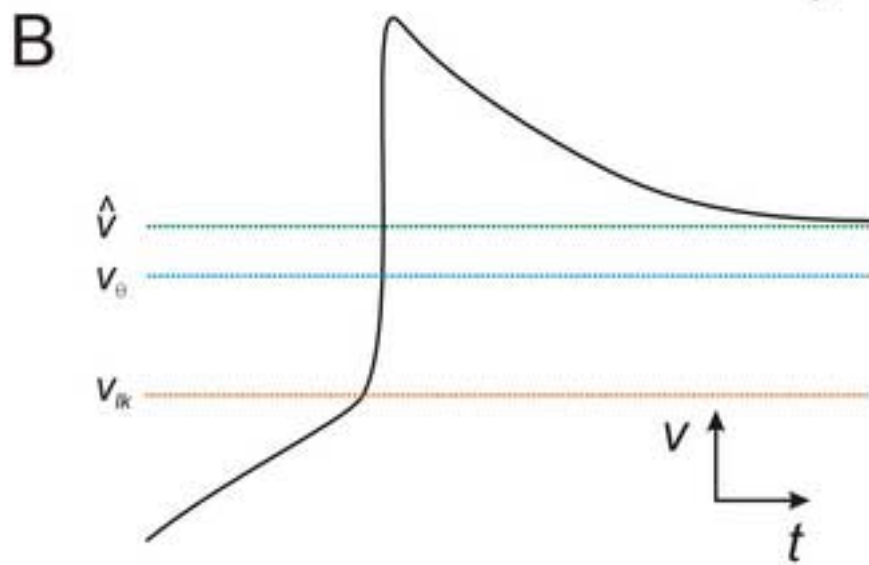
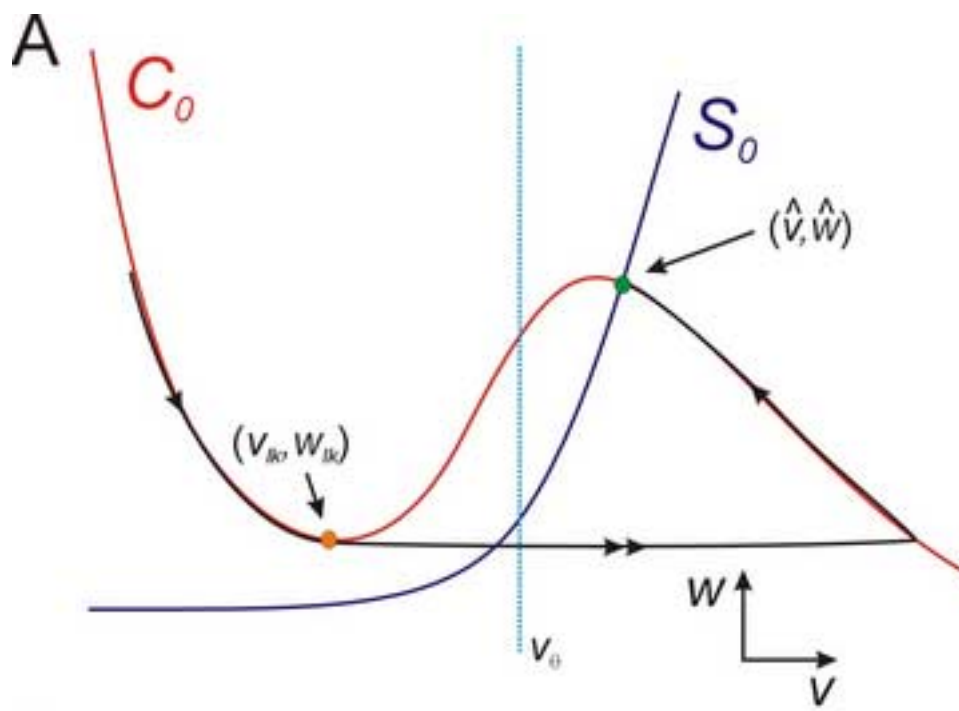


Figure 2

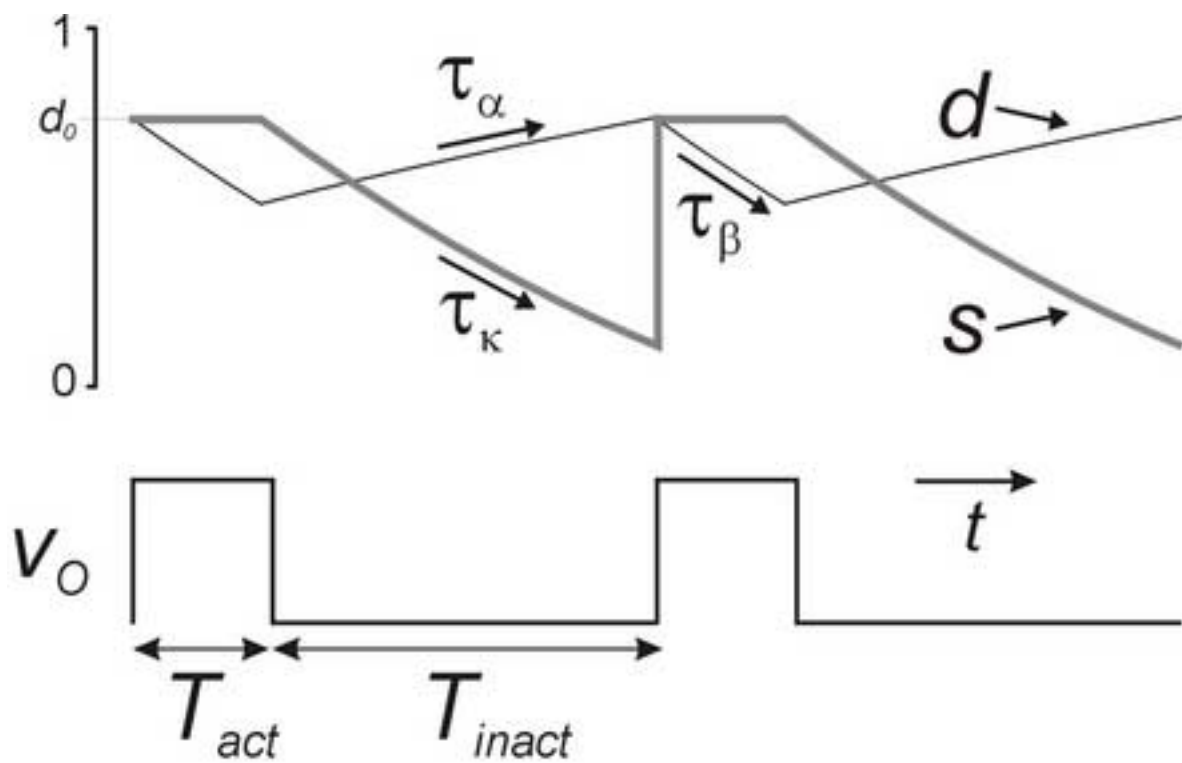


Figure 3

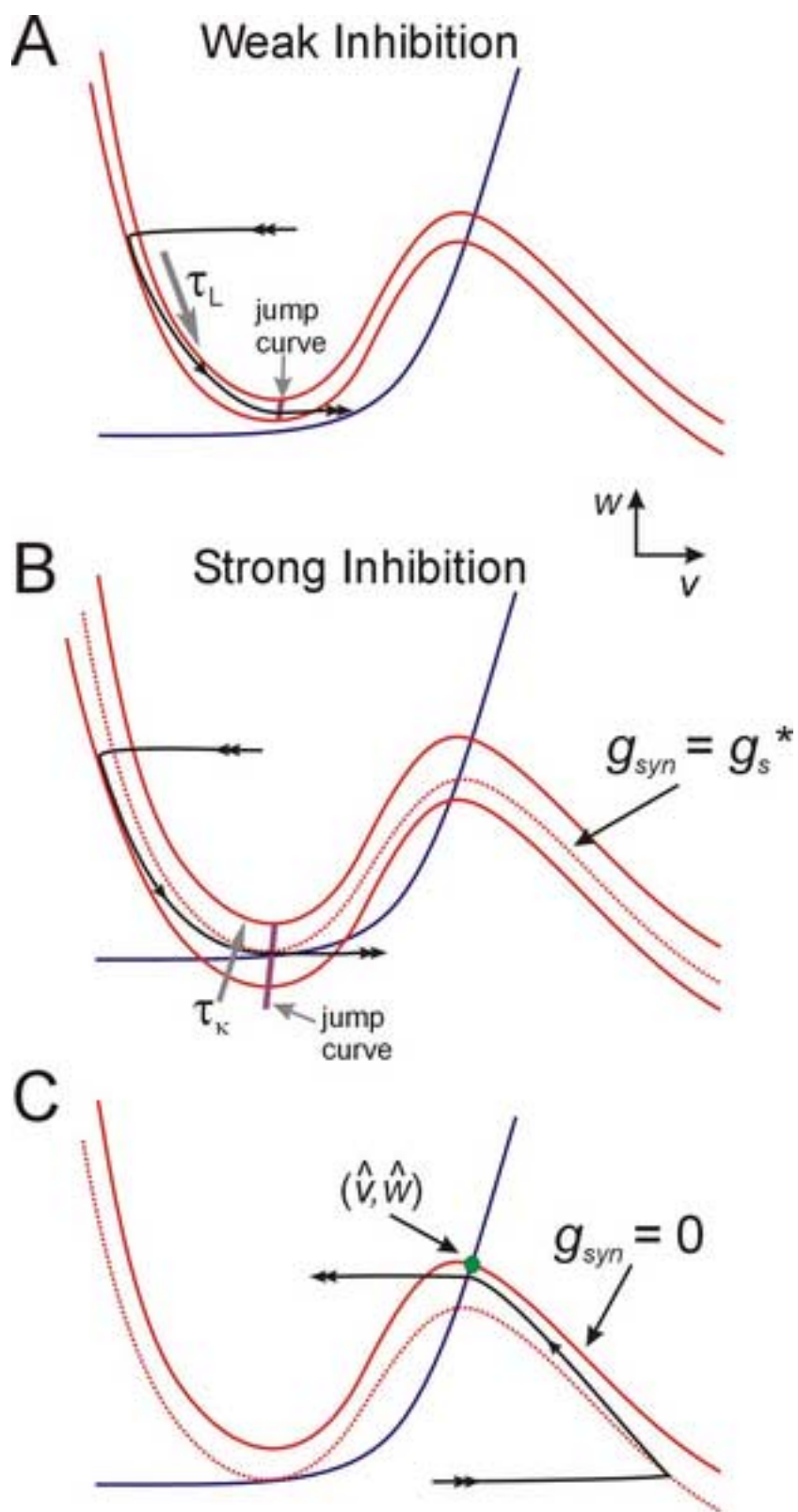


Figure 4

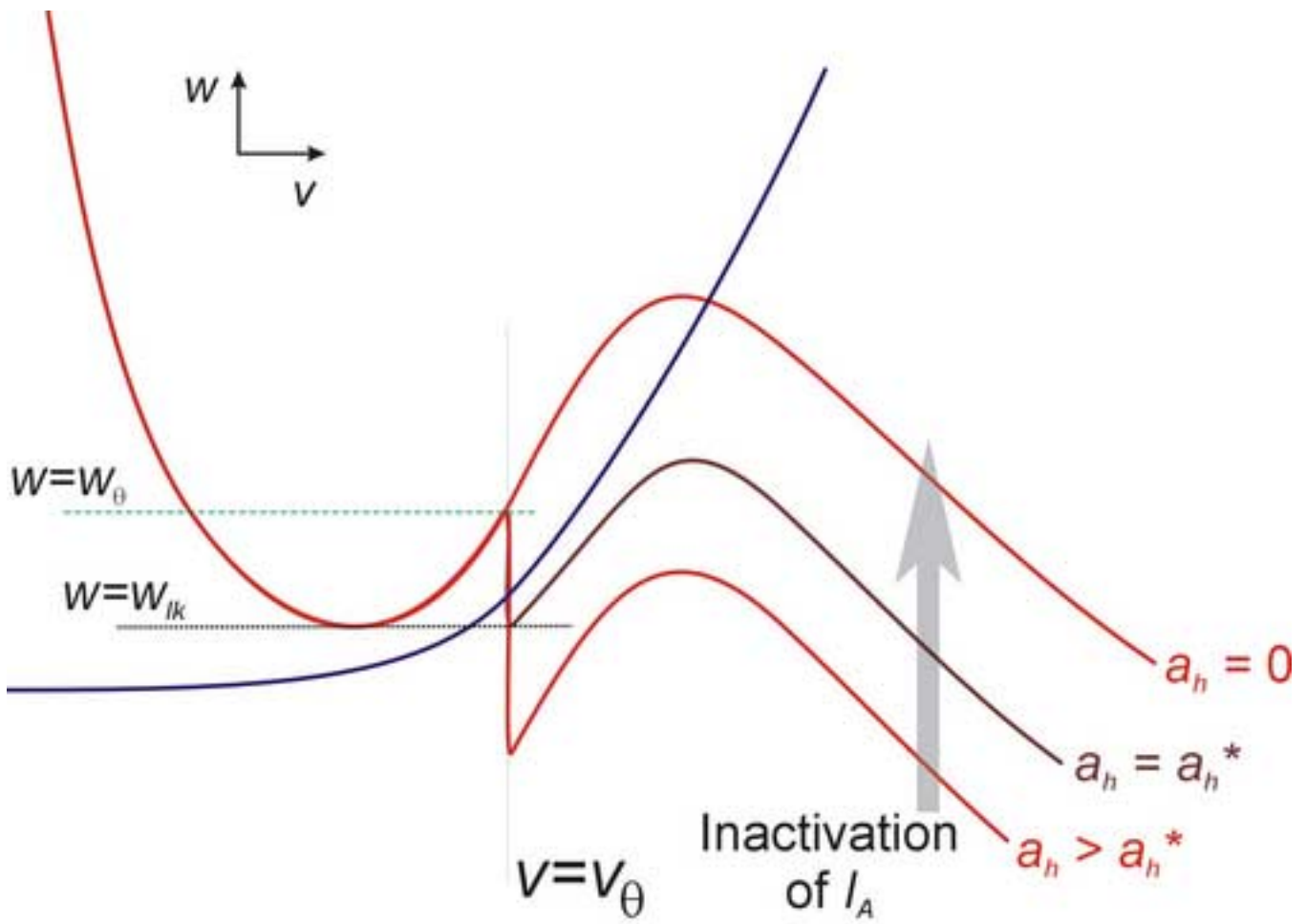


Figure 5

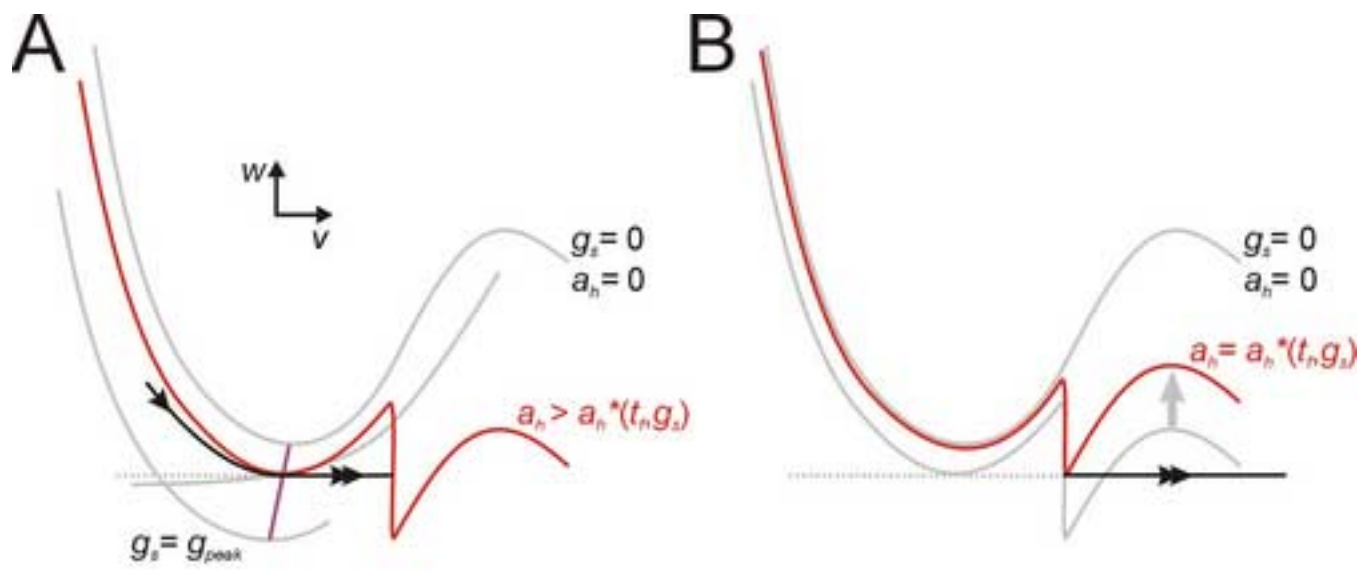


Figure 6

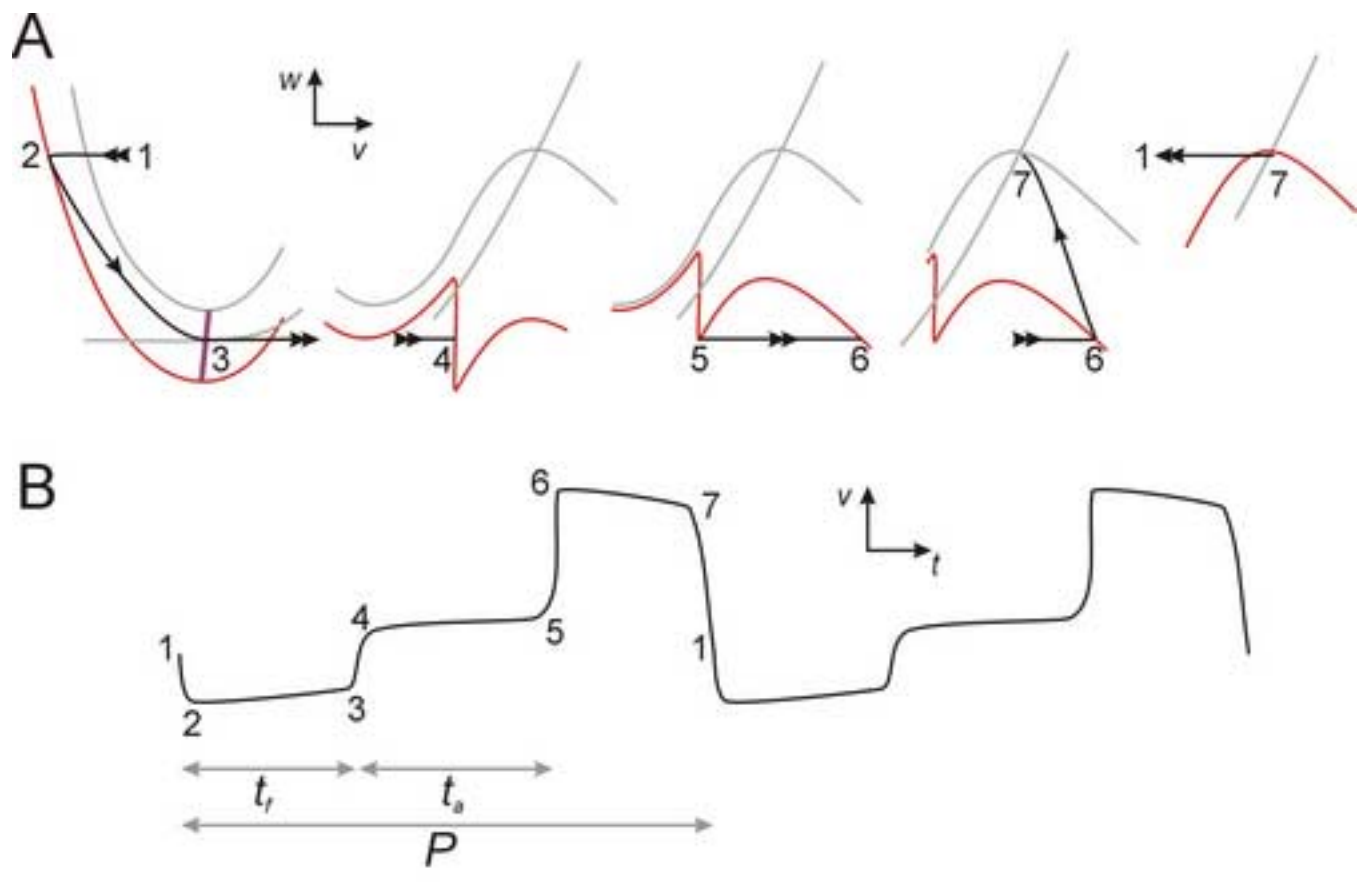


Figure 7

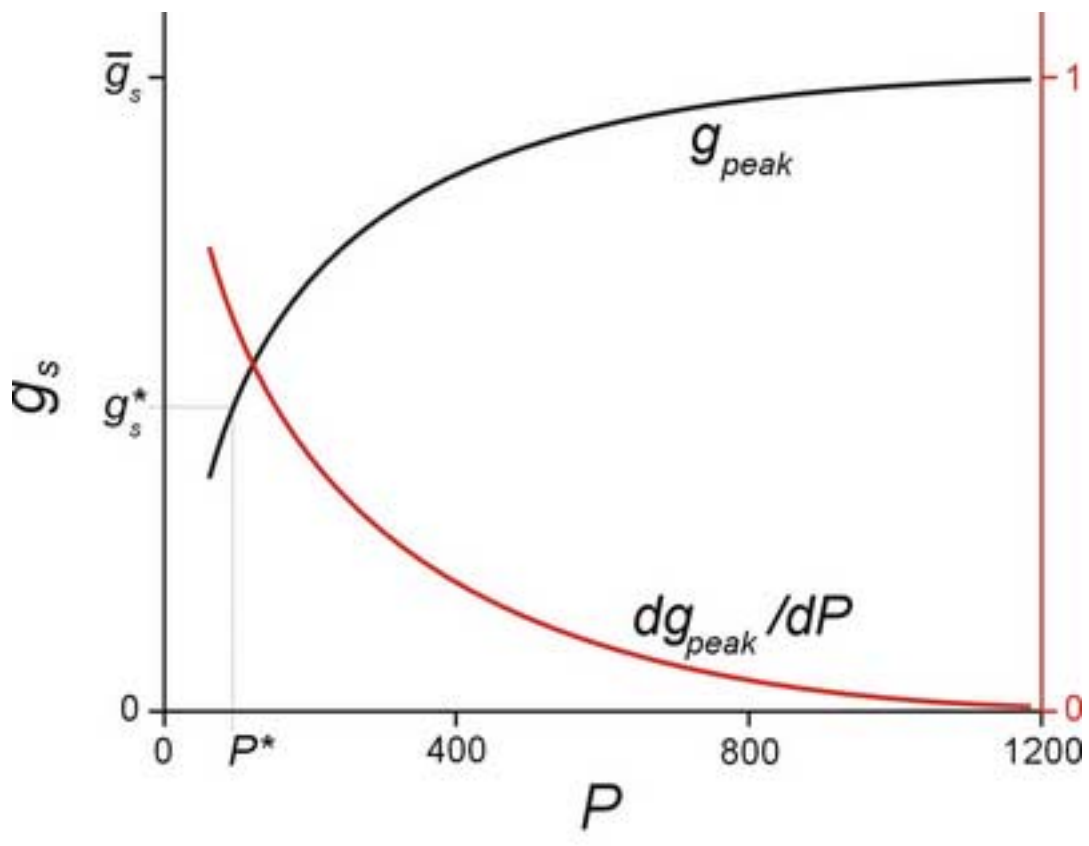


Figure 8

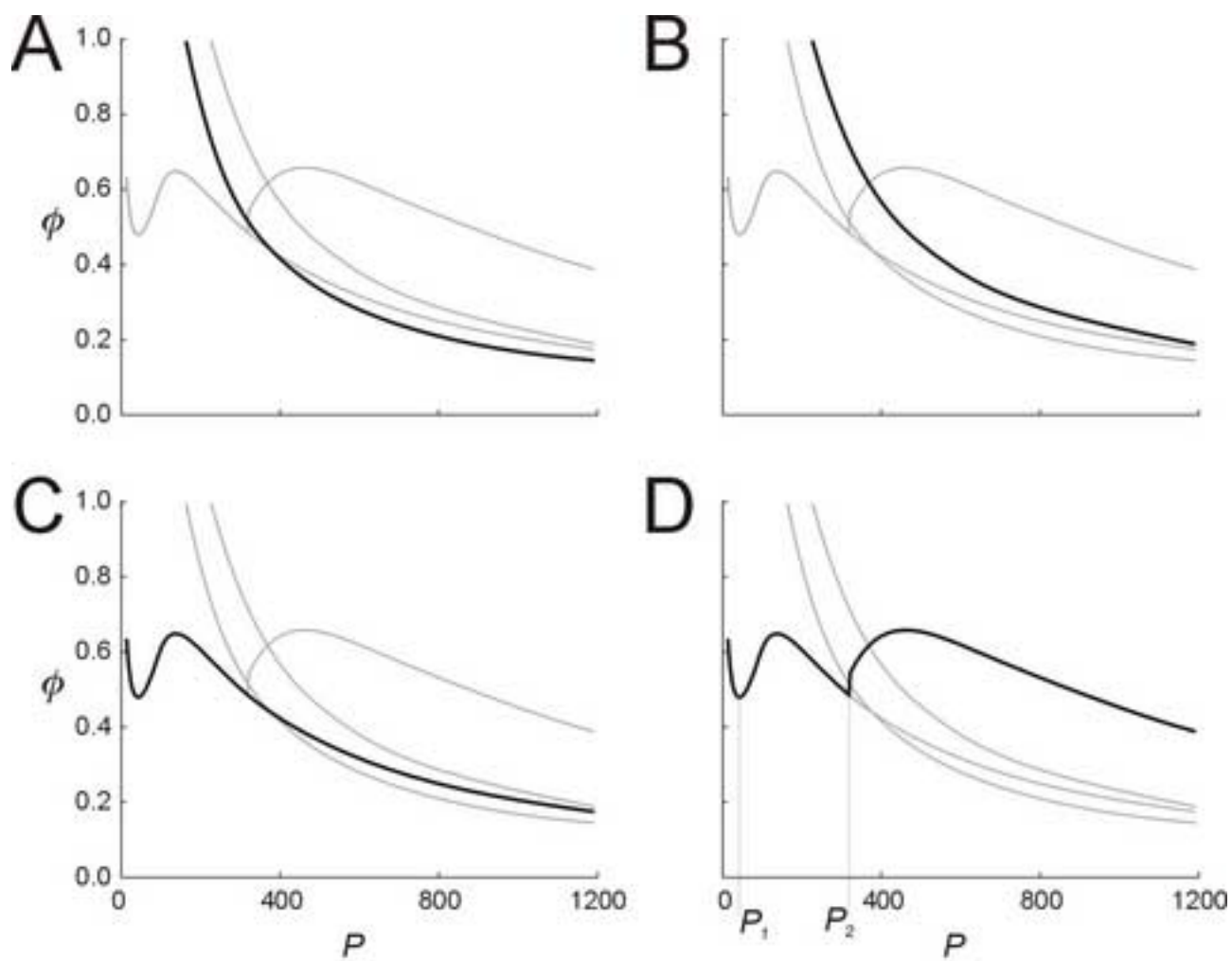


Figure 9